

Influence of Shear on Protein Crystallization under Constant Shear Conditions

Stroobants, Sander; Callewaert, Manly; Krzek, Marzena; Chinnu, Sudha; Gelin, Pierre; Ziemecka, Iwona; Lutsko, James F.; De Malsche, Wim; Maes, Dominique

Published in:
Crystal Growth and Design

DOI:
[10.1021/acs.cgd.9b01584](https://doi.org/10.1021/acs.cgd.9b01584)

Publication date:
2020

Document Version:
Accepted author manuscript

[Link to publication](#)

Citation for published version (APA):
Stroobants, S., Callewaert, M., Krzek, M., Chinnu, S., Gelin, P., Ziemecka, I., Lutsko, J. F., De Malsche, W., & Maes, D. (2020). Influence of Shear on Protein Crystallization under Constant Shear Conditions. *Crystal Growth and Design*, 20(3), 1876-1883. <https://doi.org/10.1021/acs.cgd.9b01584>

Copyright

No part of this publication may be reproduced or transmitted in any form, without the prior written permission of the author(s) or other rights holders to whom publication rights have been transferred, unless permitted by a license attached to the publication (a Creative Commons license or other), or unless exceptions to copyright law apply.

Take down policy

If you believe that this document infringes your copyright or other rights, please contact openaccess@vub.be, with details of the nature of the infringement. We will investigate the claim and if justified, we will take the appropriate steps.

Supporting information: The influence of shear on protein crystallization under constant shear conditions

Sander Stroobants,^{*,†} Manly Callewaert,[‡] Marzena Krzek,[†] Sudha Chinnu,[†] Pierre Gelin,[‡] Iwona Ziemecka,[‡] James F. Lutsko,[¶] Wim De Malsche,[‡] and Dominique Maes^{*,†}

[†]*Structural Biology Brussels, Vrije Universiteit Brussel, Pleinlaan 2, 1050 Brussel, Belgium*

[‡]*μFlow group, Department of Chemical Engineering Vrije Universiteit Brussel, Pleinlaan 2, 1050 Brussels, Belgium*

[¶]*Center for Nonlinear Phenomena and Complex Systems, Université Libre de Bruxelles, Boulevard du Triomphe, 1050 Brussels, Belgium*

E-mail: Sander.Stroobants@vub.be; Dominique.Maes@vub.be

Contents

- Figure 1: Crystal detection algorithm and example
- Figure 2: Confirmation of purity by DLS
- Figure 3: COMSOL simulations at the inlet
- Figure 4: COMSOL simulations of the concentration profile
- Figure 5: GUI designed for this application

- Figure 6: CAD files of the chip holder
- Figure 7: 3D view of the chip holder
- Figure 8: Raw data for the nucleation rate as a function of shear rate
- Figure 9: Raw data for the nucleation rate as a function of shear time

Crystal Detection

To quantize our results, we need to accurately detect crystals in the images. Utilizing MATLAB and the image processing toolbox a crystal detection algorithm was developed. The first step is to apply an edge detection algorithm based on the Canny operator. The resulting binary map can be used for segmenting the image by calculating which regions are fully surrounded by an edge in the binary image. The different segments are then saved along with additional data like the number of pixels, the centroid of the segments and the pixels which make up the segment. Beside the number of crystals, their size and shape can be automatically determined (but was not used in the described application).

The algorithm consists of the following steps.

1. Crop picture to 800 by 800 pixels
2. Improve sharpness of the image (`imsharpen`) and equalize the histogram (`adapthisteq`) to improve the contrast
3. Use Canny edge detection, the output is a black and white image:
`BW = edge(Image, 'Canny', [0.15 0.20])`
4. Dilate the detected edges: `imdilate`
5. Fill in the holes made by the edges: `imfill`
6. Make a list off all the connected regions: `bwconncomp`

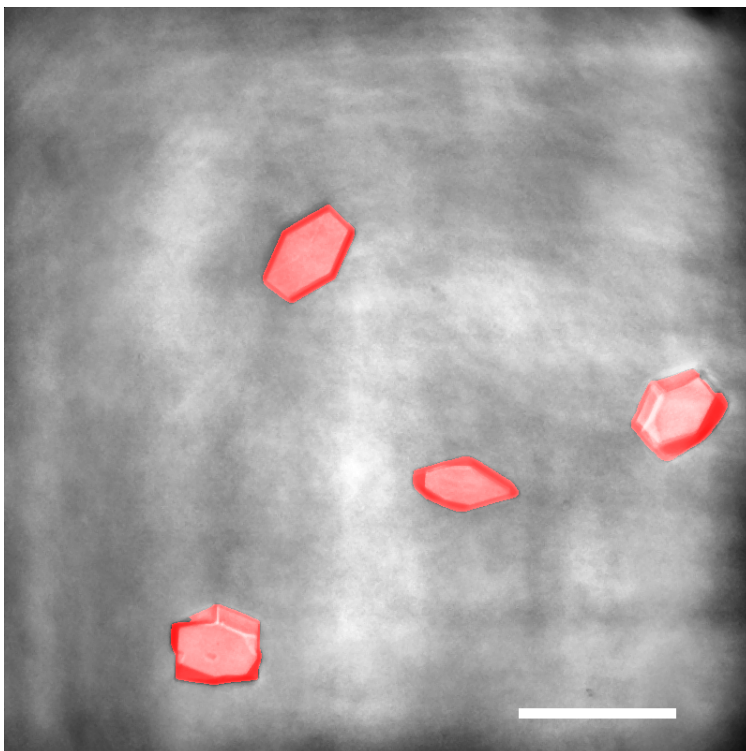


Figure 1: Example of the results from the crystal detection algorithm. The detected crystals are marked in red.

7. Calculate properties (area, bounding box, etc) of the different regions: `regionprops`

One of the drawbacks of this method is that very small crystals (< 5 pixels) are difficult to detect. To account for this inaccuracy all images were manually inspected. Figure 1 shows an example of the results from the algorithm.

Confirmation of purity by DLS

Dynamic light scattering was used to verify that the shearing experiments and device don't introduce any impurities to the sample during operation. Pure water (milli Q) was injected into the device. Samples were collected at the outlet after filling of the device and after shearing was completed. The correlation curves are shown in Figure 2. No shoulders were present in any of the samples, confirming that no impurities were present in the water samples and that the experimental and cleaning methods used are adequate to ensure pure operation.

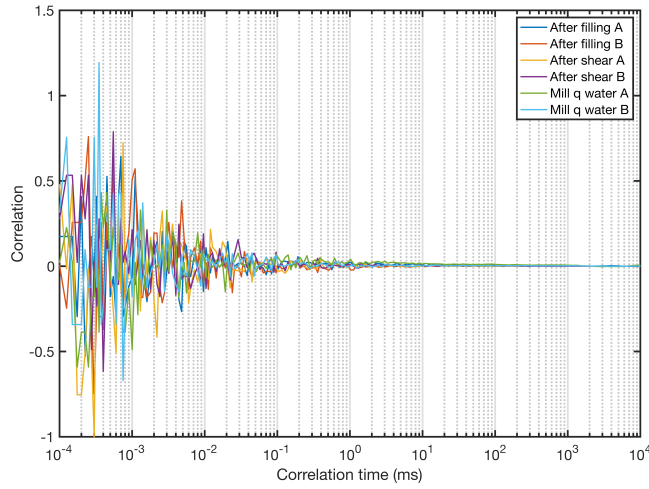


Figure 2: DLS measurements of pure water. Samples were taken after filling and after shearing. No shoulders are visible in the correlation curves confirming that no impurities were introduced by shearing.

COMSOL simulations

The effect of the inlets was simulated with COMSOL multiphysics. The disruption of the flow and shear profile, caused by the inlets, are localized in the intimate vicinity of the inlet (see Figure 3). To be sure that these small deviations do not affect the results no images from in neighbourhood of the inlet were analyzed.

By using the “transport of diluted species” module in COMSOL we also investigated the influence of shear on the concentration profile of lysozyme inside the channel. We found no deviations larger than 0.2% from a homogeneous concentration profile for the concentrations used in the paper and shear rates up to 100 s^{-1} (see figure 4).

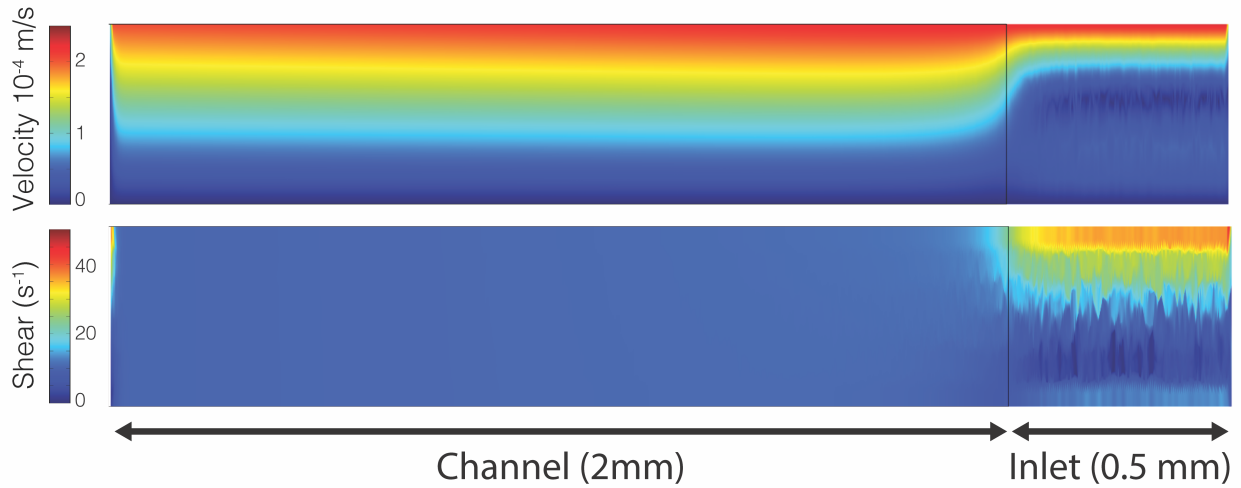


Figure 3: Velocity and shear profile in the channel and the effect of the inlet. Position of the cross section is indicated in Figure 3 in the article.

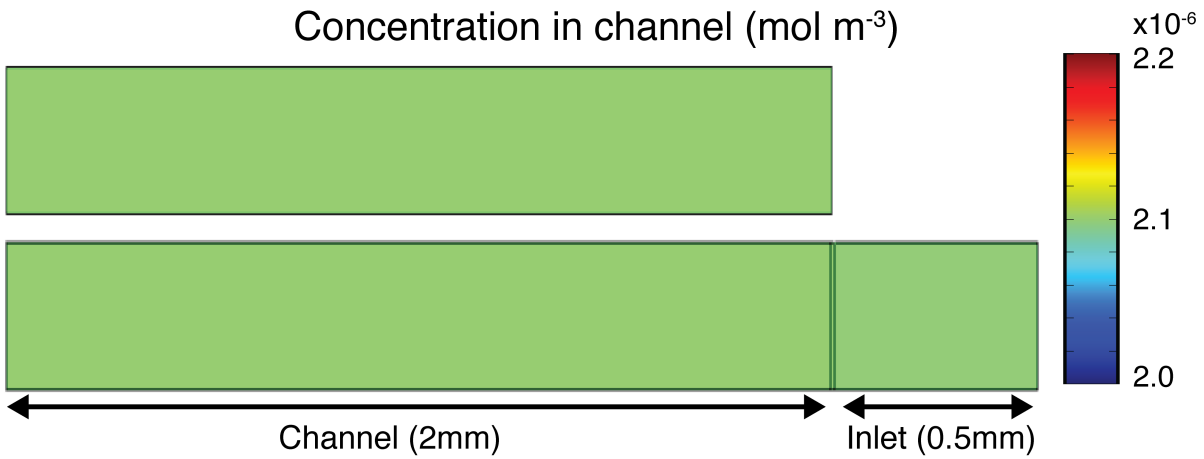


Figure 4: Concentration profile of lysozyme inside the channel during shearing. Made with COMSOL. Top: Channel without inlet. Bottom: Channel with inlet. No deviations larger than 0.2% are detectable compared to a homogeneous solution. A lysozyme concentration of 30 mg ml^{-1} (with a molecular weight of lysozyme of 14307 Da) is equal to $2.1 \times 10^{-6} \text{ mol m}^{-3}$. A diffusion coefficient of $5 \times 10^{-11} \text{ m}^2 \text{s}^{-1}$ is used and a shear rate of 100 s^{-1} .

Extra figures

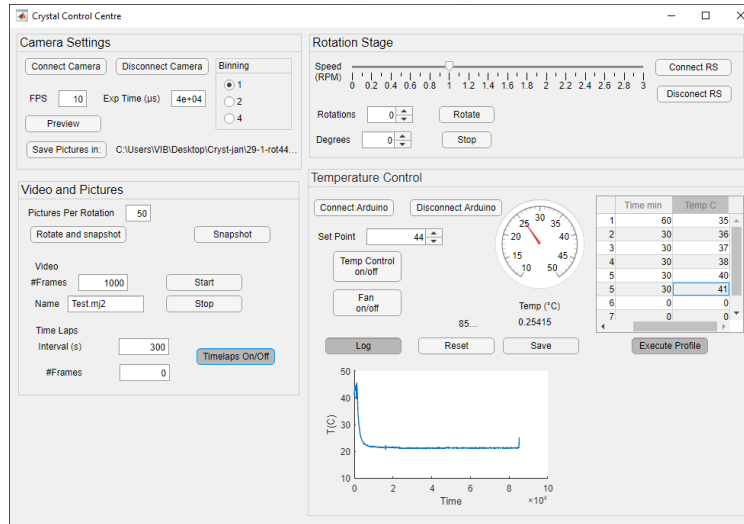


Figure 5: The graphical user interface used to control the temperature, activation of the rotation stage and the camera enabling precise, simultaneous and intuitive use of the different subsystems.

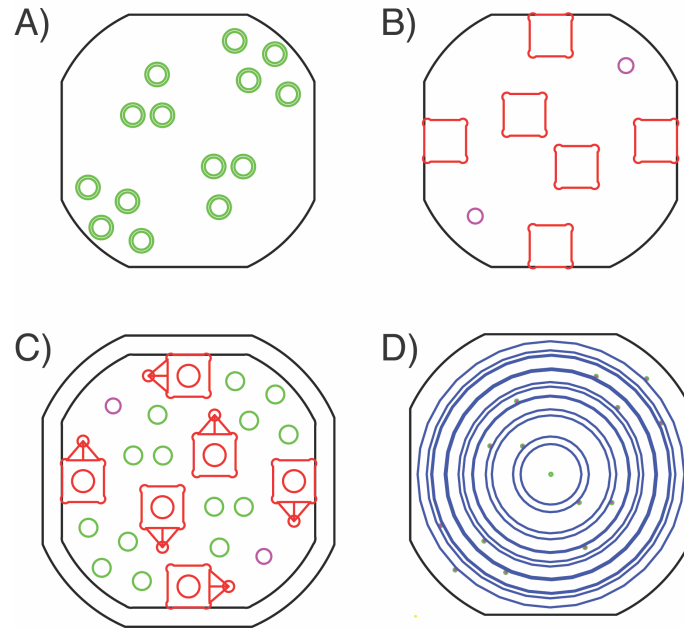


Figure 6: CAD drawings for the different parts of the device: A) top of the aluminium plate, B) bottom of aluminium plate, C) Delrin holder, D) mask used for wet etching of the microfluidic chip. Green represents the wholes for the nanoports, red the cavities for the peltier elements and purple the cavities for the temperature sensor.

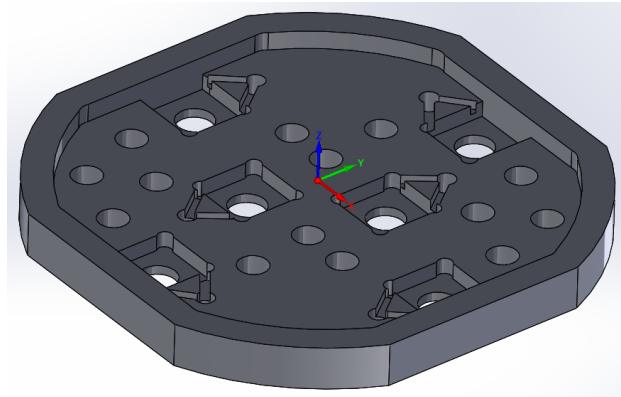


Figure 7: 3D view of the model for the Delrin holder.

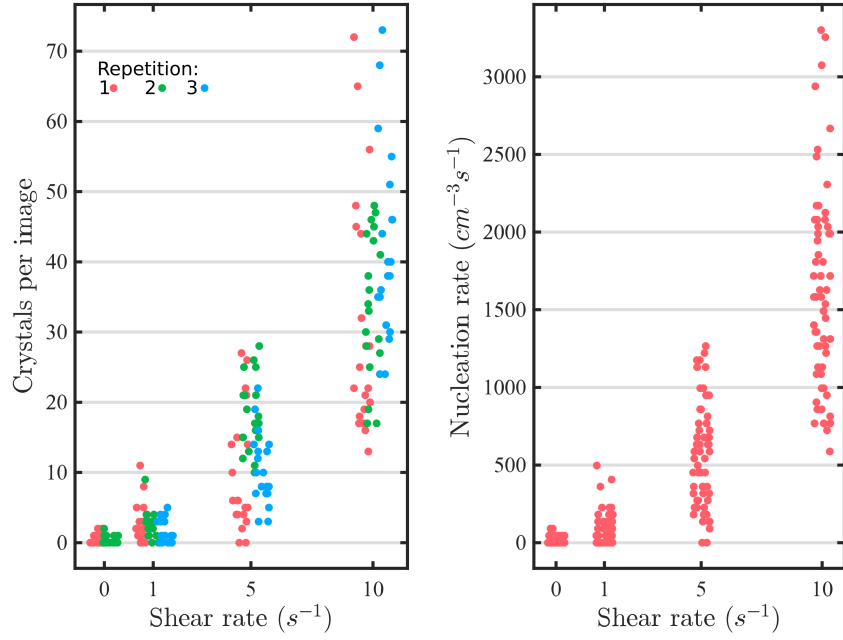


Figure 8: The raw data used for Figure 10 in the paper. Scatter plot of the nucleation data as a function of shear rate. Each dot represents the results of 1 picture. Left: Crystals per image as a function of shear rate. The different repetitions are depicted in red, blue and green. Right: Nucleation rate as a function of shear rate. All repetitions are taken together.

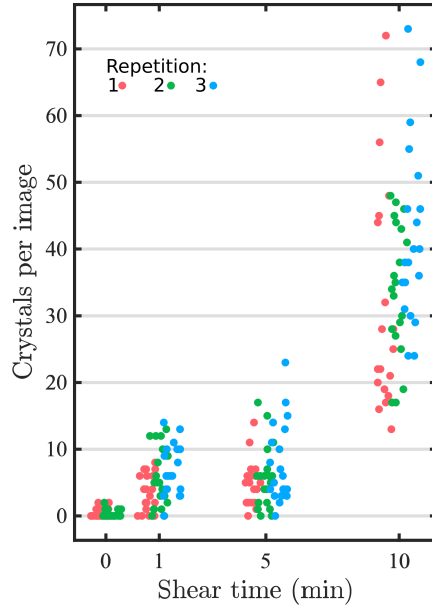


Figure 9: The raw data used for Figure 11 in the paper. Scatter plot of the nucleation data as a function of shear time, each dot represents the results of 1 picture. Crystals per image as a function of shear rate. The different repetitions are depicted in red, blue and green.